

# Approaching the Atrium Through the Intraparietal Sulcus: Mapping the Sulcal Morphology and Correlating the Surgical Corridor to Underlying Fiber Tracts

Christos Koutsarnakis, MD\*<sup>†</sup>

Faidon Liakos, MD\*<sup>†</sup>

Aristotelis V. Kalyvas, MD,  
MSc\*<sup>†</sup>

Evangelia Liouta, MSc<sup>‡</sup>

John Emelifeonwu, MD\*

Theodosios Kalamatianos,  
PhD<sup>§</sup>

Damianos E. Sakas, MD, PhD\*<sup>‡</sup>

Elizabeth Johnson, PhD<sup>||</sup>

George Stranjalis, MD, PhD\*<sup>‡</sup><sup>†</sup>

\*Department of Clinical Neurosciences, Western General Hospital, Edinburgh, UK;

<sup>‡</sup>Department of Neurosurgery, University of Athens, Evangelismos Hospital, Athens, Greece; <sup>§</sup>Hellenic Center for Neurosurgical Research "Petros Kokkalis," Athens, Greece; <sup>†</sup>Microneurosurgery Laboratory, Evangelismos Hospital, Athens, Greece; <sup>||</sup>Laboratory of Education and Research in Neurosciences, Department of Anatomy, University of Athens, Athens, Greece

#### Correspondence:

Christos Koutsarnakis, MD,  
Department of Clinical Neurosciences,  
Western General Hospital,  
Crewe Rd S,  
Edinburgh EH4 2XU, United Kingdom.  
E-mail: ckouts@hotmail.co.uk

Received, December 1, 2015.

Accepted, December 13, 2016.

Published Online, February 27, 2017.

Copyright © 2017 by the Congress of  
Neurological Surgeons

**BACKGROUND:** Although the operative corridor used during the intraparietal transsulcal approach to the atrium has been previously investigated, most anatomical studies focus on its relationship to the optic radiations.

**OBJECTIVE:** To study the intraparietal sulcus (IPS) morphology and to explore the subcortical anatomy with regard to the surgical trajectory used during the intraparietal transsulcal tranventricular approach.

**METHODS:** Twenty-five adult, formalin fixed, cerebral hemispheres were investigated. Fifteen underwent the Klingler procedure and were dissected in a lateromedial direction using the fiber microdissection technique. The trajectory of the dissection resembled that of real operative settings. The remaining 10 hemispheres were cut along the longitudinal axis of the sulcus in order to correlate its surface anatomy to corresponding parts of the ventricular system.

**RESULTS:** IPS demonstrated an interrupted course in 36% of the specimens while its branching pattern was variable. The sulcus anterior half was found to overly the atrium in all occasions. Four discrete, consecutive white matter layers were identified en route to the atrium, ie, the arcuate fibers, the arcuate segment of the superior longitudinal fasciculus, the corona radiata and tapetum, with the arcuate segment being near to the dissection trajectory.

**CONCLUSION:** Given the angle of brain transgression during the intraparietal approach, we found the optimal dissection area to be the very middle of the sulcus. The IPS–postcentral sulcus meeting point, in contrast to previous thought, proved to risk potential injury to the arcuate segment of the superior longitudinal fasciculus, thus affecting surgical outcome.

**KEY WORDS:** Atrium, Fiber dissection technique, Intraparietal sulcus, Microsurgical anatomy, Transsulcal approaches, White matter anatomy

*Operative Neurosurgery* 13:503–516, 2017

DOI: 10.1093/ons/owp037

**S**urgical access to the atrium of the lateral ventricle remains a challenge. This is not only attributed to its deep location, but also to the inherent relation of the atrium to adjacent eloquent neurovascular structures.<sup>1</sup> Selection of surgical approach for the management of atrial lesions varies according to their size, extent, pathology, and

vascularity, as well as the surgeon's experience, the patient's preoperative neurological assessment and hemispheric dominance.<sup>2-7</sup> Among the various operative variants in ventricular trigone surgery currently available, one of the most commonly advocated is the intraparietal transsulcal approach, during which a direct and effective operative corridor is accomplished through the roof of the atrium. Since this region of the atrium is devoid of fibers of the optic radiation,<sup>3,6,8-11</sup> this approach, at least theoretically, does not risk damage to visual areas, and hence, effectively avoids common complications

**ABBREVIATIONS:** DTI, diffusion tensor imaging; IPS, intraparietal sulcus; MRI, magnetic resonance imaging; 3-D, three dimensional

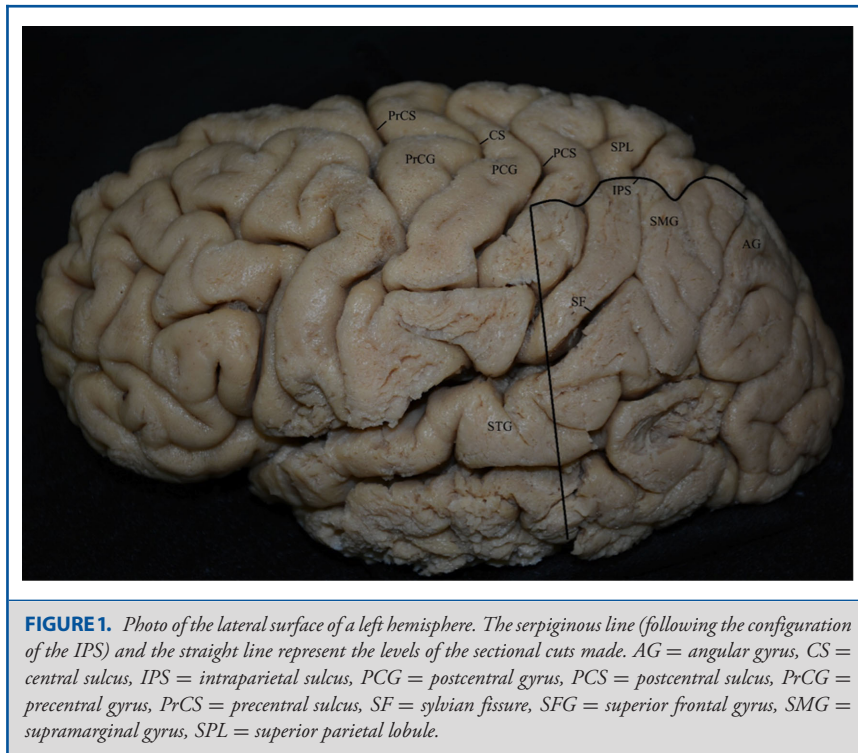


**FIGURE 1.** Photo of the lateral surface of a left hemisphere. The serpiginous line (following the configuration of the IPS) and the straight line represent the levels of the sectional cuts made. AG = angular gyrus, CS = central sulcus, IPS = intraparietal sulcus, PCG = postcentral gyrus, PCS = postcentral sulcus, PrCG = precentral gyrus, PrCS = precentral sulcus, SF = sylvian fissure, SFG = superior frontal gyrus, SMG = supramarginal gyrus, SPL = superior parietal lobule.

attributed to atrial ventricular surgery. The latter is further augmented with the integration of modern neuroimaging techniques, such as diffusion tensor imaging (DTI) and neuronavigation, which enable neurosurgeons to plan a safe trajectory through a minimal incision and craniotomy.

Despite the apparent advantages of the intraparietal transsulcal approach, the high morphological variability of the intraparietal sulcus (IPS) and the tight correlation of the surgical corridor to eloquent subcortical white matter pathways appear to have been underestimated. While several studies have demonstrated the course of the optic radiation and its relation to the walls of the atrium,<sup>3,8-15</sup> there is little evidence regarding the morphology of the IPS and its relation to the underlying fiber tracts, other than the bundles of the optic radiation, across the operative trajectory applied during the intraparietal transventricular approach. Even with the assistance of advanced neuroimaging methods, these anatomic and surgical ambiguities have not been adequately addressed.

The purpose of this study was to examine the detailed surface anatomy of the IPS, as well as to assess the complex relationships of the intraparietal transsulcal corridor to the proximal subcortical white matter pathways, using fiber microdissection technique in formalin-fixed brain specimens. To our knowledge, this is the first white matter laboratory examination of this confined brain region, which aims to provide a detailed 3-dimensional (3-D) appreciation of the cortical and subcortical anatomy relevant to surgical practice.

## METHODS

The study included 25 normal, adult cerebral hemispheres previously fixed in a 10% to 15% formalin solution for a minimum period of 6 weeks. Following careful removal of the arachnoid membrane and vessels, we thoroughly investigated and recorded the course, configuration, length, and depth of the IPS in all specimens. The IPS was defined as the most prominent sulcus on the lateral surface of the parietal lobe, originating from the postcentral sulcus and terminating at the point where it meets the imaginary line running between the extension of the parietooccipital sulcus to the superolateral cerebral surface and the preoccipital notch. This line demarcates the parietal from the occipital lobe.

Special attention was given to the branching pattern of the 2 typical rami arising from the IPS, namely the inferiorly situated intermediate sulcus of Jensen and the superiorly directed transverse parietal sulcus of Brissaud.<sup>16-19</sup>

Initially, 15 cerebral hemispheres underwent the Klingler procedure (freeze-thaw procedure)<sup>20</sup> and were explored using the fiber dissection technique and the microscope (Carl Zeiss OPMI<sup>R</sup> Plus, Carl Zeiss AG, Oberkochen, Germany).<sup>21</sup> Following identification of the IPS, we applied the aforementioned technique to the brain area surrounding the sulcus, ie, the superior parietal lobule and a part of the inferior parietal lobule, starting from the depth of the sulcus and gradually proceeding medially until entering the ventricular system. The dissection was extended to the superolateral surface of the occipital lobe, in order to clearly demonstrate the relationship of the optic radiation fibers to the surgical corridor associated with the intraparietal transsulcal approach to the ventricular trigone. The fiber tracts encountered during the procedure were carefully recorded, and their relation to the operative trajectory was determined.

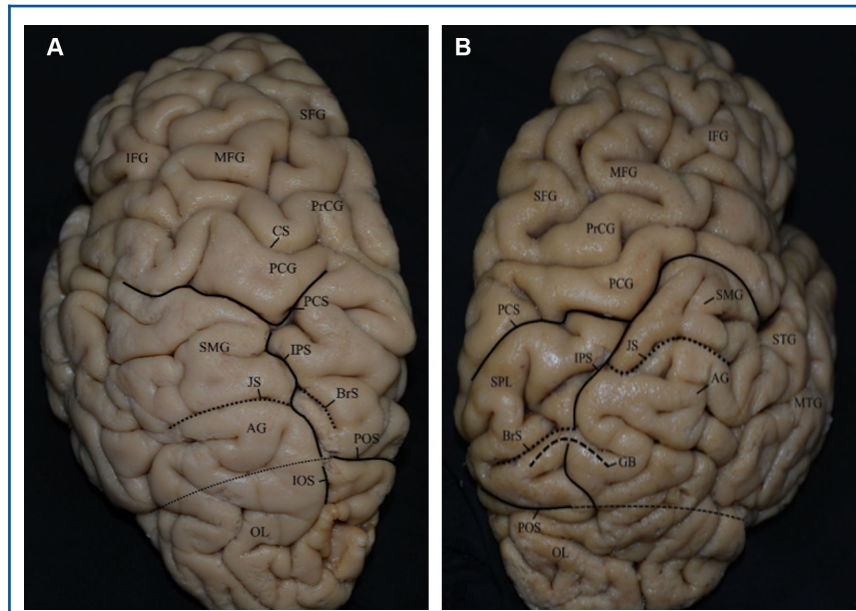


**FIGURE 2.** Morphological patterns of IPS. Two oblique photos of the lateral parietal cerebral surface of different hemispheres are illustrated in order to demonstrate the morphological variability of the IPS. **A**, The IPS in this hemisphere pursues a continuous, unbroken course toward the occipital lobe to become the intraoccipital sulcus. No superficially running gyral passage divides the sulcus. Additionally, the superiorly directed sulcus of Brissaud branches off proximal to the sulcus of Jensen. **B**, Photo of the posterolateral surface of a right cerebral hemisphere. The IPS originates from the postcentral sulcal complex and terminates at the level of the parietoccipital sulcus. Its course is almost parallel to that of the interhemispheric fissure. It is divided by a superficially running gyral bridge into a longer anterior segment and a shorter posterior segment (interrupted). In the middle of the anterior segment, the sulcus of Jensen descends to the inferior parietal lobule, separating the supramarginal from the angular gyrus. The sulcus of Brissaud also arises from the anterior segment of the IPS but distal to the Jensen's originating point and is directed superiorly. Figures 4-9 illustrate the stepwise lateromedial white matter dissection of the IPS and its adjacent cortical area of the specimen depicted in the right panel. AG = angular gyrus, BrS = sulcus of Brissaud, CS = central sulcus, GB = gyral bridge, IFG = inferior frontal gyrus, IOS = intraoccipital sulcus, IPS = intraparietal sulcus, JS = sulcus of Jensen, MFG = middle frontal gyrus, MTG = middle temporal gyrus, OL = occipital lobe, PCG = postcentral gyrus, PCS = postcentral sulcus, POS = parietoccipital sulcus, PrCG = precentral gyrus, SFG = superior frontal gyrus, SMG = supramarginal gyrus, SPL = superior parietal lobule, STG = superior temporal gyrus.

Examination of the remaining 10 hemispheres was aimed at defining the relationship of the sulcus to the atrium and to measure the respective distances from the fundus of the sulcus to the roof of the atrium. This was achieved through a sectional cut along the longitudinal axis of the IPS, which closely resembles the plane of the brain transgression carried out in the operative setting. Since the angle of the intraoperative dissection is almost perpendicular to the part of the sulcal fundus that is exposed by the surgeon each time, we recorded the relations of the different parts of the sulcus to the underlying deep anatomical structures, so as to be compatible with respect to this surgical principle. It should be stressed that although coronal cuts made at different levels of the sulcus can demonstrate the interrelationships between the sulcus and underlying deep structures, they do not resemble the actual plane of the intraoperative dissection. As such, they provide limited applied anatomical knowledge for proper intraoperative orientation. An additional cut,

perpendicular to the first and at the level of the originating point of the IPS, was also made, which allowed for a more accurate delineation of the regional anatomy (Figure 1). The dissection tools used were fine metallic periosteal dissectors, various sized anatomical forceps, and microsurgical scissors, since they proved easier and more precise to handle than the traditional described wooden spatulas.<sup>21,22</sup> We assessed (1) the morphology of the IPS, (2) the relationship of the sulcus to the ventricular trigone and other corresponding deep anatomical structures following the cut along its longitudinal axis, and (3) the white matter fiber tracts that line the parenchymal corridor between the fundus of the IPS and the atrium of the lateral ventricle. All dissections and measures were recorded with digital photographs. None of the images included in this laboratory investigation were edited by photo-enhancing software, so that they closely resemble the anatomy encountered during the dissection process.<sup>21,22</sup>

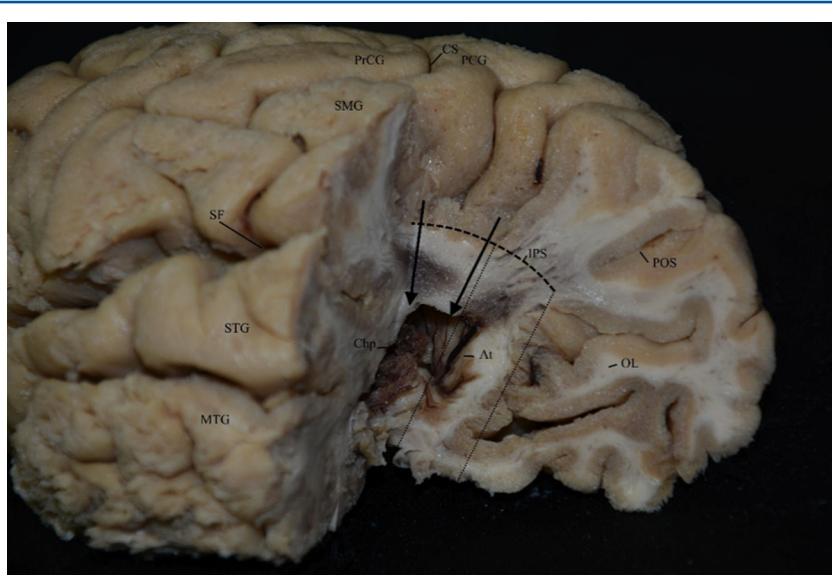


**FIGURE 3.** Corresponding deep structures with respect to IPS anterior and posterior half. A posterolateral view of hemisphere depicted in Figure 1 following the aforementioned sectional cuts. The curved dashed line represents the fundus of the IPS. Two dotted lines are drawn perpendicular to the sulcus at the middle and the end of the sulcus respectively. Given the intraoperative dissection angle, which is usually perpendicular to the sulcal fundus, the anterior half of the sulcus clearly overlies the ventricular trigone and can be safely used during the intraparietal transsulcal approach. It is evident that by moving the dissection corridor distal to the middle of the sulcus, surgical distance to the atrium is increased and safe access necessitates tilting of the operative trajectory. The anteriorly located arrow represents the dissection trajectory applied through the IPS–postcentral sulcus meeting point. The arrow located more distal along the length of the sulcus is the proposed point through which atrium's access is direct, effective and achieved without risking injury to the arcuate fasciculus (see Discussion). At = atrium, Chp = choroid plexus, CS = central sulcus, IPS = intraparietal sulcus, MTG = middle temporal gyrus, OL = occipital lobe, PCG = postcentral gyrus, POS = parietoccipital sulcus, PrCG = precentral gyrus, SF = sylvian fissure, SMG = supramarginal gyrus, STG = superior temporal gyrus.

We have also incorporated 3 axial magnetic resonance imaging (MRI) cuts and a 3-D volume rendering of the same MRI scan in order to demonstrate the proper preoperative identification of the IPS and appreciate its topography and morphology for surgical practice.

Additionally, axial and sagittal neuronavigation screen captures during presurgical planning (Stealth Station S7 Surgical Navigation system, Medtronic, Minneapolis, Minnesota) have been included, so as to vividly illustrate the surgical angle and operative corridor achieved through the intraparietal transsulcal transventricular approach. Informed consent was obtained from 2 patients prior to the inclusion of the aforementioned images to the study.

## RESULTS

### Morphology of the IPS

Based on the inspection of the cerebral surface anatomy, we found that the IPS originated from the postcentral sulcal complex in 24 out of 25 hemispheres investigated (96%). The sulcus demonstrated a continuous course in 16 (64%) hemispheres

and an interrupted course in 9 (36%) hemispheres. When the sulcus demonstrated an interrupted pattern, it was divided by a superficially running (ie, visible from the cerebral surface) gyral bridge into 2 segments, the anterior and the posterior segment. In 6 of the 9 hemispheres with an interrupted sulcus (67%), the anterior segment was larger (almost double in length) than the posterior segment, while in 2 specimens (2/9; 22%) the posterior segment was larger. The 2 segments were equal in length in only 1 hemisphere (1/9; 11%). Unexpectedly, even the 16 hemispheres that exhibited a continuous sulcal pattern demonstrated a “submerged” gyral bridge upon a wide sulcal splitting that was not initially evident on the superficial inspection of the parietal surface anatomy. In this regard, the IPS in our study sample could be considered a noncontinuous sulcus in all cases. The sulcus was parallel or almost parallel to the interhemispheric fissure in 19 specimens (76%), while in the 7 remaining hemispheres, (23%) it followed an oblique direction compared to that of the interhemispheric fissure.



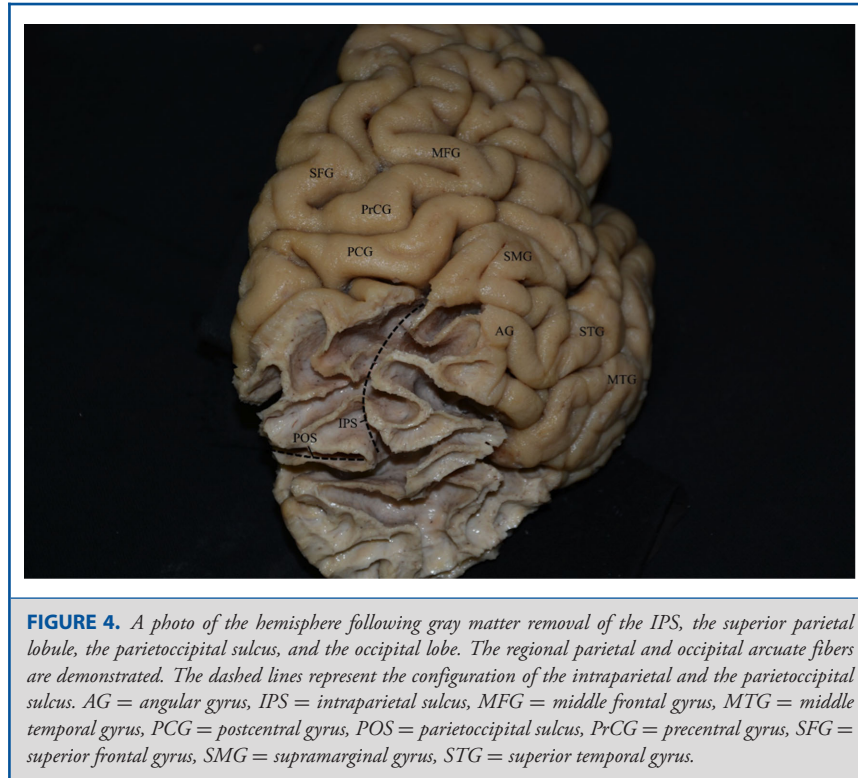


**FIGURE 4.** A photo of the hemisphere following gray matter removal of the IPS, the superior parietal lobule, the parietoccipital sulcus, and the occipital lobe. The regional parietal and occipital arcuate fibers are demonstrated. The dashed lines represent the configuration of the intraparietal and the parietoccipital sulcus. AG = angular gyrus, IPS = intraparietal sulcus, MFG = middle frontal gyrus, MTG = middle temporal gyrus, PCG = postcentral gyrus, POS = parietoccipital sulcus, PrCG = precentral gyrus, SFG = superior frontal gyrus, SMG = supramarginal gyrus, STG = superior temporal gyrus.

The branching pattern of the IPS also exhibited considerable variability. The 2 typically described rami, namely the inferiorly running intermediate sulcus of Jensen and the superiorly directed transverse parietal sulcus of Brissaud, were inconsistently present in our study sample. More specifically, in 14 hemispheres (14/25; 56%) both sulci were recognized, while in 6 (24%) and in 3 (12%) of the investigated specimens only Brissaud and Jensen were readily identified, respectively. In the remaining 2 hemispheres (8%), neither of the rami was well developed. In the 14 hemispheres where both rami were evident, the sulcus of Jensen emerged more anteriorly compared to the sulcus of Brissaud in 8 cases (57%), approximately at the same level in 5 specimens (36%), and more posteriorly in 1 hemisphere (7%).

The average length of the IPS was 4.6 cm (range: 3.2-6 cm) and its average depth was 2.0 cm (range: 1.8-2.5 cm). Several submerged “intrasulcal gyri” located on the banks of the IPS were noted when splitting the sulcus to examine the internal morphology. Examination of the “internal gyral pattern” showed a range from 3 to 7 intrasulcal gyri, with 5 gyri being the most common finding (Figure 2).

### Defining the Relationship of the IPS to the Ventricular System Via the Longitudinal Axis

The relationship of the IPS to its corresponding deep anatomical elements, particularly the ventricular system, was

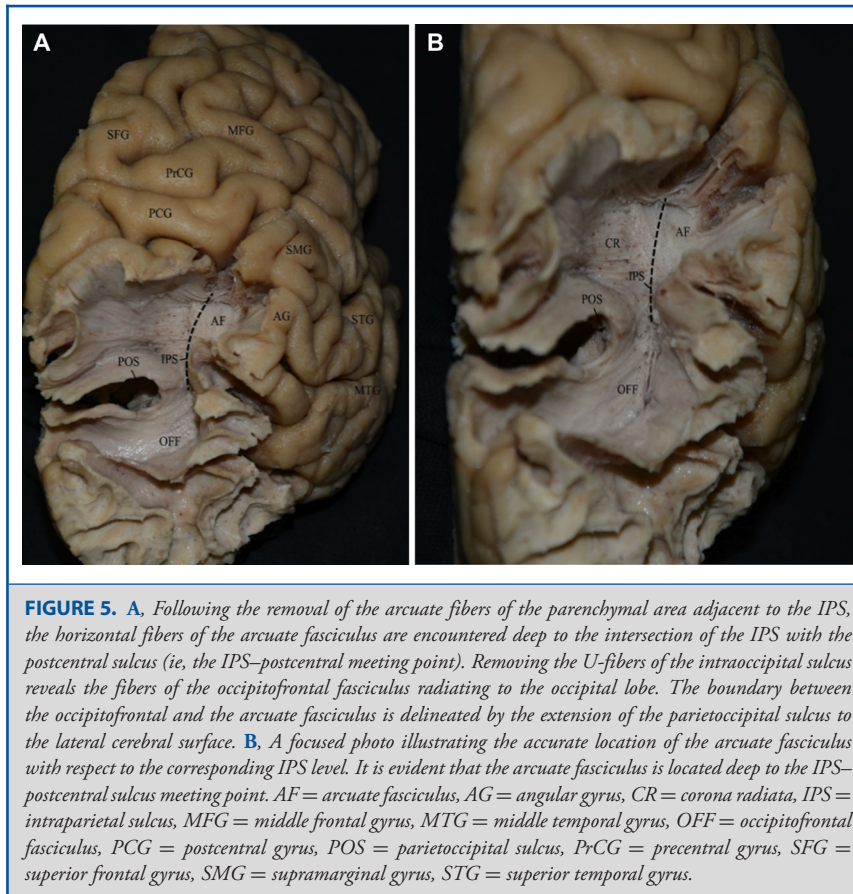
assessed via a sectional cut along the longitudinal axis of the sulcus. Observations were made with respect to the intraoperative dissection plane and trajectory used during the intraparietal transsulcal approach to access the ventricular trigone. For easier comprehension, the IPS was divided into 2 equal parts and their respective relations to the ventricular system were noted.

The anterior half of the IPS consistently lies above the atrium of the lateral ventricles in all 10 hemispheres examined (100%). A small part of the posterior half of the IPS was consistently observed above the ventricular trigone, while the majority of the posterior half was located above the occipital horn and/or the white matter of the occipital lobe in all 10 hemispheres. The distance between the fundus of the anterior half and the atrium averaged 1.25 cm (range: 0.9-2.0 cm; Figure 3).

### Anatomy of the White Matter Fiber Tracts

In order to reveal the complex fiber tract anatomy that lines the surgical corridor utilized during the intraparietal transsulcal approach to the atrium, we applied the white matter dissection technique in a stepwise lateromedial fashion. The fiber tracts encountered were categorized into 4 consecutive layers.

Peeling away the gray matter of the superior parietal lobule, part of the inferior parietal lobule, and of the superolateral occipital surface revealed the arcuate fibers that connect the aforementioned cerebral areas. These U-shaped fibers constitute the first



of the 4 previously mentioned layers (Figure 4). During this step, the cortex of the parietoccipital sulcus was also removed. This sulcus served as a useful landmark throughout the dissection procedure since, the imaginary line running between its lateral cerebral surface extension and the preoccipital notch delineates the boundary between the parietal and occipital lobes.

Dissecting the arcuate fibers at the anterior part of the IPS (ie the junction area of the sulcus to the postcentral sulcal complex) and its adjacent white matter area revealed the horizontally oriented fibers of the arcuate fasciculus. Extending the dissection into the occipital lobe and intraoccipital sulcus to the second layer, we were able to observe the posterior part of the inferior occipitofrontal fasciculus radiating to the region of the superior occipital gyrus (Figure 5). It is noteworthy that the fibers of the occipitofrontal fasciculus did not appear to extend to the white matter of the parietal lobe in any of the specimens examined. The most prominent surface landmark demarcating the superior margin of the occipitofrontal fasciculus was the part of the parietoccipital sulcus extending to the lateral cerebral surface.

Upon removal of the white matter of the second layer along the longitudinal plane of the IPS, the fibers of the corona radiata were revealed. These exhibited a characteristic ventrolateral to

dorsomedial course and comprised the third consecutive white matter layer that needed to be incised in order to enter the ventricular trigone (Figure 6). This part of the corona radiata contained fibers of the external capsule and of the retrolenticular part of the internal capsule. These functionally different fibers could not be individually dissected and recognized during this stepwise procedure, since they share the same course and direction. When the dissection was extended to the white matter of the occipital lobe and the posterior part of the occipitofrontal fasciculus was removed, the remaining fibers of the sagittal stratum could be viewed. At this level, the sagittal stratum is composed of occipitopontine and optic radiation fibers, which intermingle and cannot be properly dissected (Figure 6). As the boundary demarcating the transition from corona radiata to the sagittal stratum is the plane determined by the emerging segment of the parietoccipital sulcus to the lateral surface, this part of the parietoccipital sulcus delineates the superior extension of the optic radiation fibers and as such, guides the surgical trajectory applied during the intraparietal transsulcal approach.

Progressive dissection of the corona radiata at the level of the IPS revealed the fibers of the tapetum arching over the roof of the atrium (Figure 7). The tapetum forms the fourth and last white

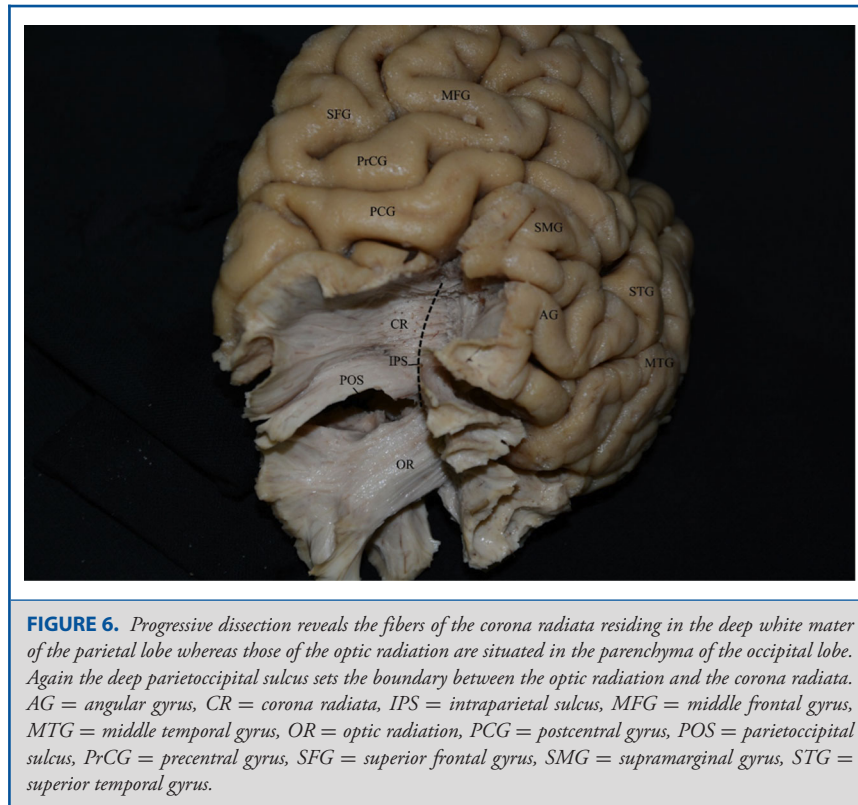


**FIGURE 6.** Progressive dissection reveals the fibers of the corona radiata residing in the deep white matter of the parietal lobe whereas those of the optic radiation are situated in the parenchyma of the occipital lobe. Again the deep parietooccipital sulcus sets the boundary between the optic radiation and the corona radiata. AG = angular gyrus, CR = corona radiata, IPS = intraparietal sulcus, MFG = middle frontal gyrus, MTG = middle temporal gyrus, OR = optic radiation, PCG = postcentral gyrus, POS = parietooccipital sulcus, PrCG = precentral gyrus, SFG = superior frontal gyrus, SMG = supramarginal gyrus, STG = superior temporal gyrus.

matter layer before the ependyma of the roof of the ventricular trigone is encountered and the atrium is entered (Figure 8). In order to accurately demonstrate the topographic relationship between the fibers of the optic radiation and the roof of the atrium, we extended the dissection to the angular gyrus and inferior parietal lobule. It was clear that the roof of the atrium was completely devoid of optic radiation fibers, which rather occupied the roof and lateral wall of the occipital horn (Figure 9). Thus, during the proper intraparietal transsulcal approach to the ventricular trigone the surgeon avoids injury to the visual pathway, where the plane determined by the parietooccipital sulcus demarcates the transition from the atrium to the occipital horn and defines the point where the optic radiation fibers sweep around the lateral wall of the atrium to reach the roof of the occipital horn.

## DISCUSSION

Arguably, the surgical utility of the cerebral sulci in accessing parenchymal brain lesions has emerged from the extension of the concept of microsurgical access of subarachnoid cisterns and major fissures, mainly proposed and propagated by Yasargil et al.<sup>23-27</sup> Meticulous dissection and opening of the sulci's arachnoid covering during transsulcal approaches shortens the surgical distance and provides adequate access while minimizing

injury to surrounding normal brain tissue.<sup>28,29</sup> In this context, the clinical application of the intraparietal transsulcal approach for accessing lesions into the atrium has aroused interest, due to the proximity and direct relationship of the sulcus to this specific part of the ventricular system.<sup>1,28,30,31</sup> According to this, following a parietal craniotomy and reflection of the dura toward the sagittal sinus, the surgeon must readily identify the IPS and its junction with the postcentral sulcal complex. Recognizing this specific anatomical landmark is mandatory, since it serves as the starting point of the sulcal dissection.<sup>18</sup> Meticulous preoperative planning regarding the proper identification of the aforementioned landmark and the course of the IPS per se on the MRI scans is a prerequisite for the optimal placement of the craniotomy site (Figures 10 and 11). The sulcal fundus can be reached following an adequate opening of the sulcus, respecting the pial planes and the vessels, allowing a cortical incision along the axis of the sulcus to be performed. The trajectory of subsequent subcortical dissection should be kept almost perpendicular to the longitudinal axis of the IPS, in order to enter the ventricular system through the roof of the atrium. This process can be assisted by image-guided stereotaxy and/or intraoperative ultrasonography. This allows the surgeon to safely and effectively access the ventricular trigone, while preserving the optic radiation, which courses on its lateral wall,<sup>3,6,9-11,15</sup> and ultimately avoid eloquent cortical motor and speech areas that lie anteriorly and laterally, respectively.<sup>2,3,6,11,30,32-34</sup>

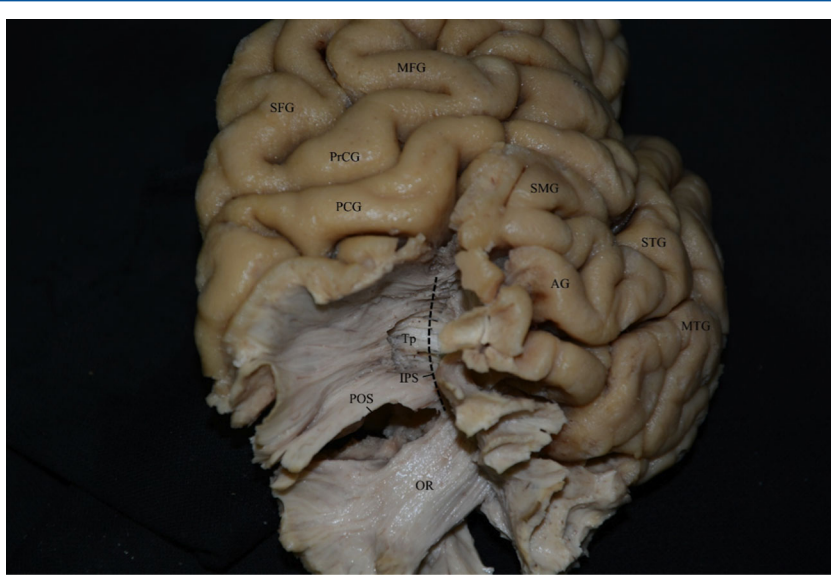


**FIGURE 7.** Dissection of the corona radiata reveals the fibers of tapetum arching over the roof of the atrium. The tapetum is the last white matter layer before entering the ventricular trigone. AG = angular gyrus, IPS = intraparietal sulcus, MFG = middle frontal gyrus, MTG = middle temporal gyrus, OR = optic radiation, PCG = postcentral gyrus, POS = parietoccipital sulcus, PrCG = precentral gyrus, SFG = superior frontal gyrus, SMG = supramarginal gyrus, STG = superior temporal gyrus, Tp = tapetum.

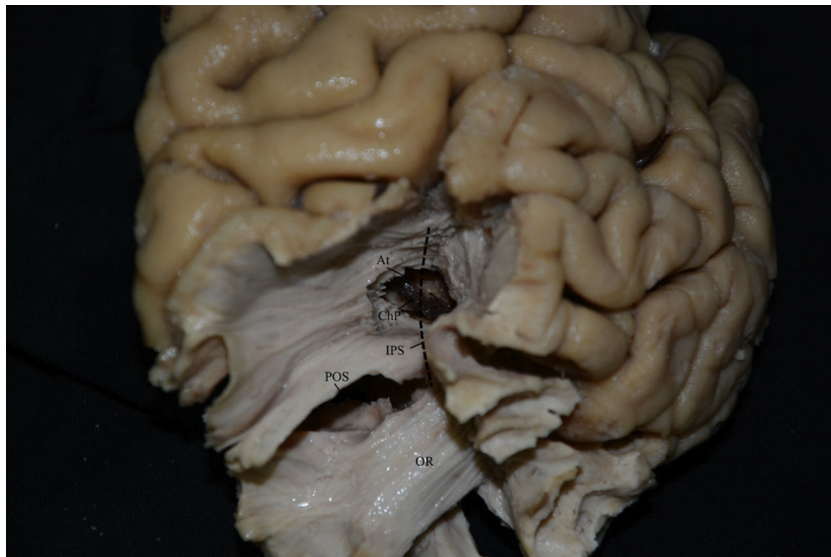


**FIGURE 8.** Removal of the tapetum discloses the roof of the atrium. The choroid plexus residing at the atrium is also apparent. At = atrium, Chp = choroid plexus, IPS = intraparietal sulcus, OR = optic radiation, POS = parietoccipital sulcus.





**FIGURE 9.** A part of the angular gyrus along with its white matter is dissected in order to expose the lateral wall of the atrium. The optic radiation fibers, which sweep around the lateral atrial wall in their way to the roof of the occipital horn, are also dissected. The black dotted line resembles the trajectory of the dissected optic fibers. Medial to the optic radiation fibers the splenial radiations course over the roof and the lateral wall of the occipital horn. At = atrium, Chp = choroid plexus, IPS = intraparietal sulcus, LWA = lateral wall of atrium, OH = occipital horn, OR = optic radiation, POS = parietoccipital sulcus, SR = splenial radiations.

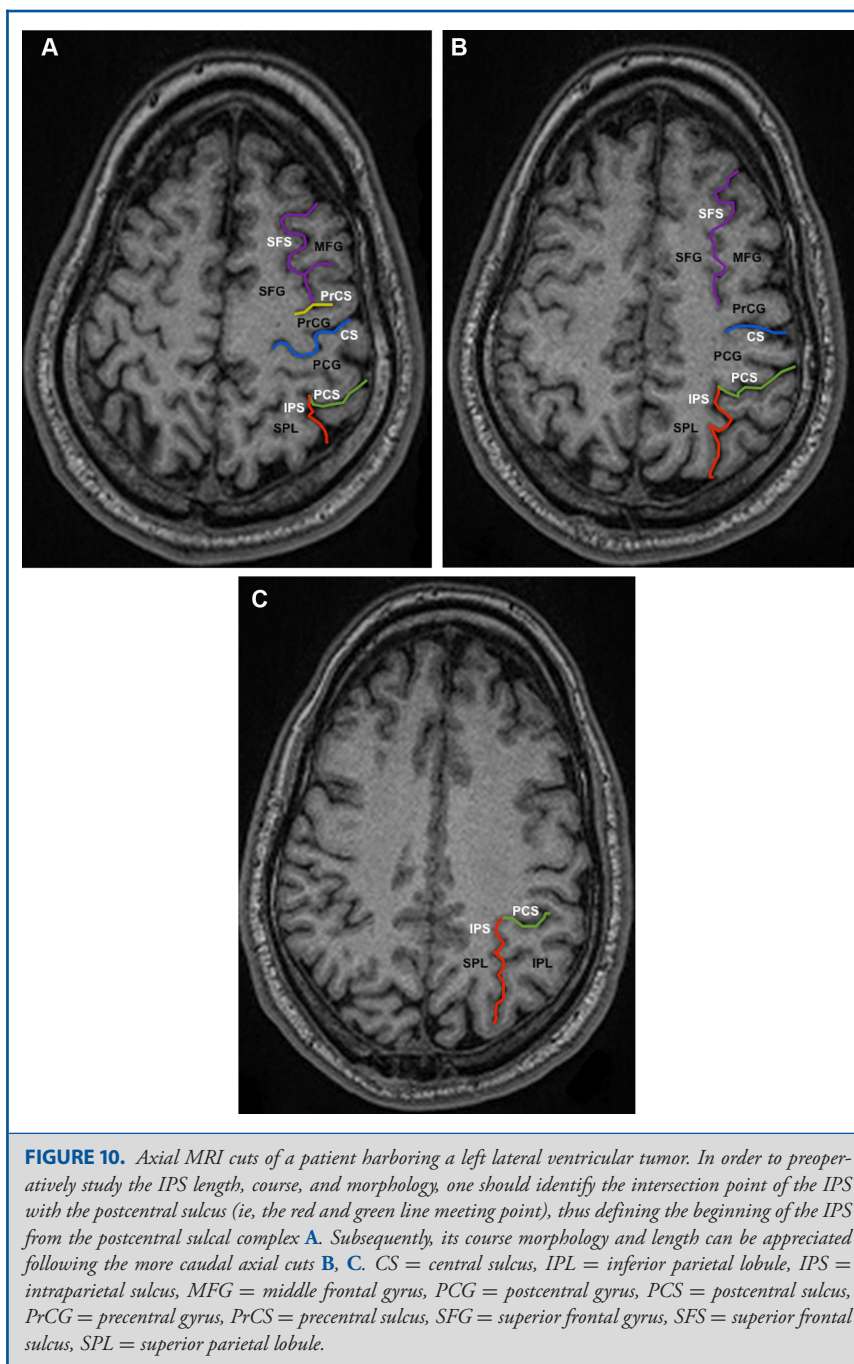
However, modern neurosurgical literature has currently underestimated 2 key elements that substantially influence the dissection process required for this approach and potentially affect the surgical outcome. These include the morphology of the IPS and the anatomical relations of the applied surgical corridor to the underlying fiber tracts, other than the visual pathways.

According to “standard neuroanatomical literature,”<sup>19,35-42</sup> the IPS originates from the postcentral sulcus and follows a continuous course to the occipital lobe, where it becomes the transverse occipital sulcus. It runs parallel to the interhemispheric fissure and gives off 2 main branches, namely the inferiorly running intermediate sulcus of Jensen and the superiorly directed transverse parietal sulcus of Brissaud.<sup>18,30</sup> Nevertheless, this anatomical pattern of the IPS tends to be oversimplistic and runs the risk of being inaccurate. Anatomical and imaging studies of the parietal lobe have previously suggested the considerable variability of the IPS morphology.<sup>16,30,43</sup> Our results, along with recent reports,<sup>17,44</sup> further support that the IPS is not always a continuous sulcus as previously thought, but rather shows an inconsistent branching pattern.

We report that the sulcus is interrupted and divided into 2 segments by a superficially running gyral bridge in 37% of the specimens studied. In the majority of cases, the anterior segment was larger, almost double in size, than the posterior

segment. The “internal morphology” of the sulcus that was revealed following arachnoid dissection was always interrupted by a submerged gyral passage, which was not visible by immediate cerebral surface inspection. These findings are consistent with recent evidence deriving from morphological studies using MRI methods aiming to elucidate structure to function relations in human brain.<sup>17,44</sup> These observations are of surgical significance, indicating that neurosurgeons must be prepared to encounter an “intrasulcal gyrus” during an intraoperative dissection of what initially appeared to be a continuous sulcus on the exposed parietal surface. Additionally, the branching pattern of the IPS exhibits considerable variability. The 2 typically described rami of Jensen and Brissaud<sup>18,19</sup> are not always present and demonstrate variable location with respect to each other.

Furthermore, since the intraparietal transsulcal approach necessitates inevitable brain transgression en route to the trigone, the surgeon should be familiar with the relevant subcortical white matter anatomy and its functional significance.<sup>4,45-47</sup> More specifically and by using the fiber microdissection technique, we were able to distinguish 4 discrete consecutive layers lining the operative corridor of the intrasulcal approach. The first layer consisted of the arcuate “U” fibers that connect adjacent gyri. The second layer comprised the arcuate segment of the superior longitudinal fasciculus, which is located deep to the most anterior part



of the sulcus. The third consecutive layer was formed by fibers of the external capsule and retrolenticular part of the internal capsule that intermingle and compose what is known as the corona radiata. At this anatomical plane, the retrolenticular limb of the internal capsule consists of parietopontine fibers. Finally, the fourth and last white matter layer, before encountering the

ventricular ependyma and entering the trigone, was the tapetum. This bundle is formed by splenial callosal radiations, which course over the roof and lateral wall of the atrium.

While the brain transgression that is required to access the ventricular trigone during this approach may involve potential injury to all of these subcortical pathways, the most significant

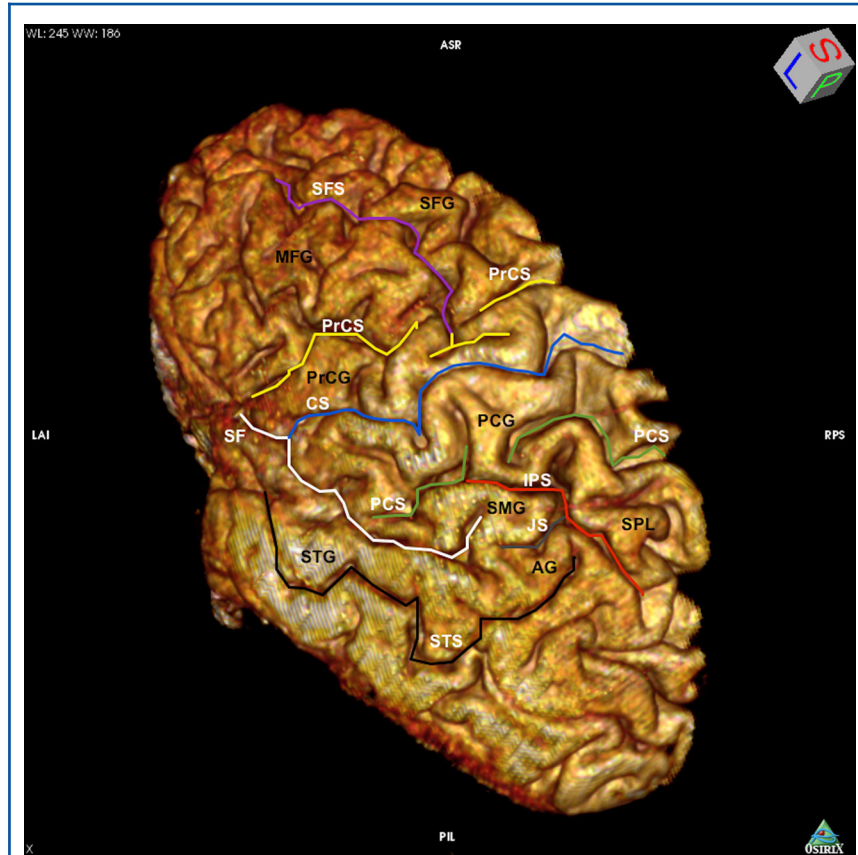


**FIGURE 11.** The 3-D volume rendering of the MRI scan in Figure 10 demonstrates a superolateral view of the left hemisphere. Three-dimensional volume rendering can be safely used as a preoperative planning tool for the intraparietal transsulcal approach since one can accurately delineate the boundaries, course, morphology, and branching patterns of the IPS. The course, morphology, and length of the IPS can be appreciated. The sulcus of Jensen (gray line) arising from the middle of the IPS and separating the angular for the supramarginal gyrus is also evident. AG = angular gyrus, CS = central sulcus, IPS = intraparietal sulcus, JS = sulcus of Jensen, MFG = middle frontal gyrus, PCG = postcentral gyrus, PCS = postcentral sulcus, PrCG = precentral gyrus, PrCS = precentral sulcus, SF = sylvian fissure, SFG = superior frontal gyrus, SFS = superior frontal sulcus, SMG = supramarginal gyrus, SPL = superior parietal lobule, STG = superior temporal gyrus, STS = superior temporal sulcus. The 3-D volume rendering image was acquired using the OsiriX application.

of these, functionally, is the arcuate segment of the superior longitudinal fasciculus given the fact that the functional significance of parietopontine<sup>48</sup> and tapetal fibers is as yet largely unknown. However, regarding the tapetum there is increasing evidence arising from DTI studies that it is implicated in the complicated process of language comprehension.<sup>49,50</sup> With regard to the arcuate segment of the superior longitudinal fasciculus studies using intraoperative direct subcortical stimulation of the parenchymal area corresponding to this fiber tract elicited paraphasias and repetition disorders in the dominant hemisphere, thus documenting its pivotal role in the so-called perisylvian language pathway.<sup>45,51-55</sup> Accordingly, subcortical stimulation in

the nondominant hemisphere elicited vestibular symptoms, such as nystagmus and vertigo, suggesting its implication in audiovisuospatial processing and spatial awareness.<sup>47,56</sup>

This suggests that especially with lesions in the dominant hemisphere, the dissection plane should be kept within the anterior half of the intraparietal segment, which consistently overlies the atrium, but distal to the IPS–postcentral sulcus meeting point, in order to avoid injury to the arcuate fasciculus. While the IPS–postcentral sulcus meeting point has been found in neuroanatomic reports to be a safe and effective starting point of the intraoperative dissection during this approach,<sup>28,30</sup> most of these studies have investigated the anatomical evidence mainly

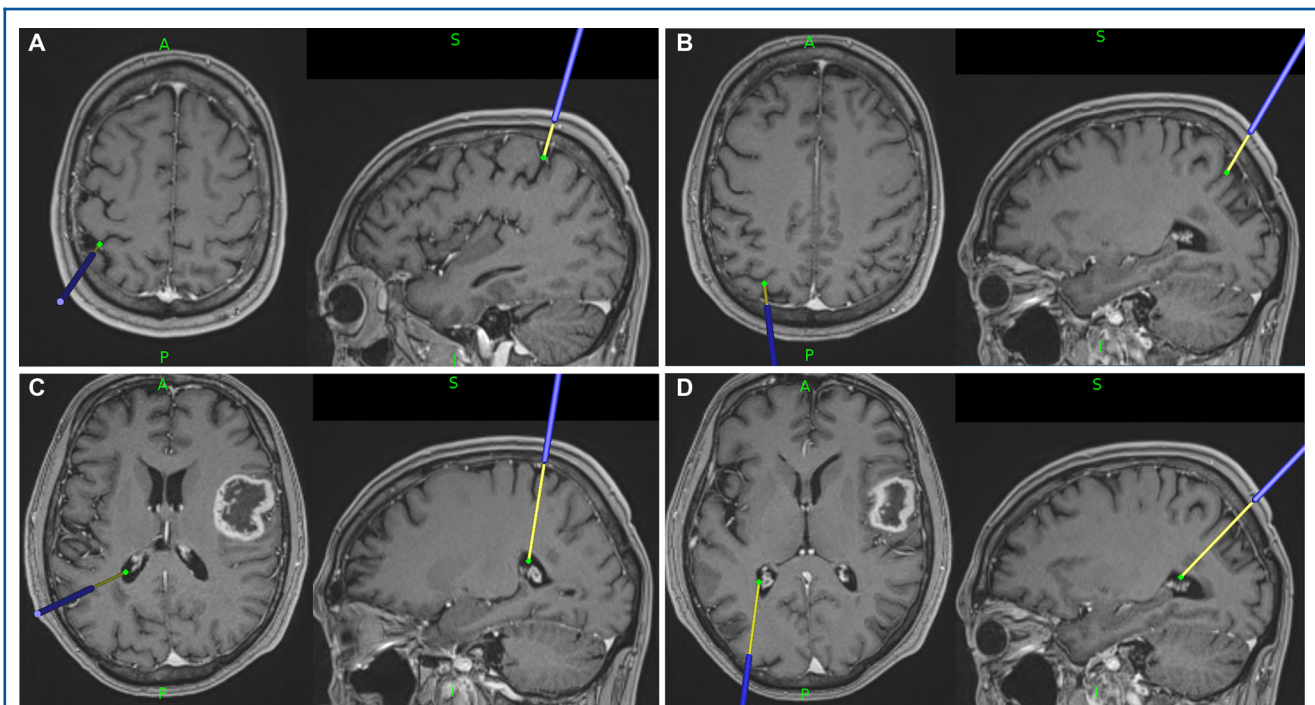


**FIGURE 12.** Axial and sagittal views obtained from a standard navigation system (Stealth station S7 Surgical Navigation system, Medtronic), during preoperative planning for the resection of a right-sided ring-enhancing lesion, demonstrating on the left side: **A** the IPS–postcentral sulcus meeting point (the standard starting point for the cortical and subcortical dissection during the intraparietal transsulcal approach). **B**, The point approximately at the middle of the sulcus—the “mid-IPS point” (the new proposed starting point for cortical and subcortical dissection, which avoids injuring the arcuate fasciculus). **C**, The “IPS–postcentral” trajectory to the atrium of the left lateral ventricle. **D**, The “mid-IPS” trajectory to the atrium of the left lateral ventricle. The angle of the surgical trajectory and therefore the direction of the respective operative subcortical dissection through the “mid-IPS point” is much more tilted in the sagittal plane when compared to the one achieved through the standard IPS–postcentral sulcus meeting point. This is expected since the proposed “mid-IPS point” is located more posteriorly along the sulcal length and thus along the cranial convexity. This can be also appreciated in Figure 3, where the IPS is correlated to its deep corresponding ventricular segments.

from the cerebral surface morphology and from coronal cuts, without exploring the regional subcortical fiber tract architecture. The results from this study suggest that the safest dissection area along the length of IPS is the region lying at the very middle of the sulcus with a slight anterior projection, since this would preserve the adjacent eloquent cortical (sensorimotor cortex) and subcortical anatomy. The relevant anatomic correlates and subcortical dissection trajectories of the aforementioned proposed modification as compared to the current approach, through the IPS–postcentral sulcus meeting point, are vividly illustrated in Figure 12.

Regarding the functional significance of the cortex buried within the IPS, ie, the sulcal fundus and lateral banks, that the surgeon has to either traverse or retract during the approach, accumulating evidence suggests its implication in saccadic eye movements,<sup>57</sup> attention,<sup>57,58</sup> episodic memory retrieval,<sup>58</sup> and multimodal processing of visual, auditory, tactile, and motion stimuli.<sup>57</sup> Specifically, the cortex of the anterior part of the lateral bank of the IPS in both hemispheres plays a significant role in visual-guided grasping movements.<sup>57,59–62</sup>

Additionally, special attention should be paid to the functional significance of the nondominant parietal lobe, which although is not traditionally considered as an eloquent area indeed clinical syndromes resulting from its injury can hugely affect patient's quality of life. Nondominant parietal lobe lesions are mainly associated with contralateral visuospatial neglect,<sup>63</sup> visual-motor ataxia,<sup>64,65</sup> and some forms of apraxia such as dressing and constructive apraxia.<sup>66,67</sup> Emphasis should be placed on the so called “contralateral neglect” which is defined as the inability to perceive stimuli on one side of the body or environment with otherwise intact visual acuity, somatic sensation, and motor function.<sup>66,68–71</sup> This neuropsychological condition is mainly observed in lesions of the nondominant inferior parietal lobule<sup>68</sup> and can negatively affect the patient's functional recovery. Interestingly, the right parietal lobe mediates attention to both left and right visual hemifields, whereas the left hemisphere mediates attention only to the right visual field.<sup>66</sup> Hence, left parietal lesions tend to be compensated by the intact right hemisphere and rarely result in hemineglect.<sup>66</sup> It is worth mentioning that patients experiencing hemineglect rehabilitate much longer and



are less likely to live independently than patients with dominant hemisphere damage.<sup>72</sup>

In summary, the intraparietal transsulcal approach to the atrium offers a direct and effective operative corridor, while reducing the surgical distance and minimizing brain transgression when compared to current transcortical transventricular operative variants. Wide opening of the sulcus and proper planning of the dissection angle enable adequate exposure with minimal brain retraction. Despite the apparent effectiveness of this approach, particular emphasis must be placed on the morphological diversity of the IPS (Figure 10) and on the complex regional underlying white matter anatomy with respect to the applied surgical trajectory. In addition to a detailed understanding of this intricate neuroanatomy, prerequisites for successful surgery and optimal patient outcome also demand meticulous neurophysiological preoperative assessment, visual field testing, thorough evaluation of the preoperative MRI scans, and knowledge of the implementation of intraoperative image-guided stereotaxis and/or ultrasonography.

## CONCLUSION

By mapping the pattern of the IPS and by exploring the respective white matter anatomy in detail, this study identified that the optimal point for the cortical incision and brain transgression en route to the ventricular trigone is the middle and anterior half of the sulcus, but clearly away from the meeting point of the IPS with the postcentral sulcus. According to the authors' view, this surgical maneuver, since avoiding injury to the arcuate fasciculus, reduces the risk of postoperative language deficits and constructional apraxia, thus lowering operative morbidity, while maintaining an efficient intraoperative field for surgical manipulation.

## Disclosure

The authors have no personal, financial, or institutional interest in any of the drugs, materials, or devices described in this article.

## REFERENCES

- Rhoton AL Jr. The lateral and third ventricles. *Neurosurgery*. 2002;51(4 suppl):S207-S271.
- D'Angelo VA, Galarza M, Catapano D, Monte V, Bisceglia M, Carosi I. Lateral ventricle tumors: surgical strategies according to tumor origin and development—a series of 72 cases. *Neurosurgery*. 2005;56(1 suppl):ONS-36-ONS-45.
- Kawashima M, Li X, Rhoton AL Jr, Ulm AJ, Oka H, Fujii K. Surgical approaches to the atrium of the lateral ventricle: microsurgical anatomy. *Surg Neurol*. 2006;65(5):436-445.
- Martino J, De Witt Hamer PC, Berger MS, et al. Analysis of the subcomponents and cortical terminations of the perisylvian superior longitudinal fasciculus: a fiber dissection and DTI tractography study. *Brain Struct Funct*. 2013;218(1):105-121.
- McDermott MW. Intraventricular meningiomas. *Neurosurg Clin N Am*. 2003;14(4):559-569.
- Nayar VV, DeMonte F, Yoshor D, Blacklock JB, Sawaya R. Surgical approaches to meningiomas of the lateral ventricles. *Clin Neurol Neurosurg*. 2010;112(5):400-405.
- Nayar VV, Foroosan R, Weinberg JS, Yoshor D. Preservation of visual fields with the inferior temporal gyrus approach to the atrium. *J Neurosurg*. 2009;110(4):740-743.
- Peltier J, Travers N, Destrieux C, Velut S. Optic radiations: a microsurgical anatomical study. *J Neurosurg*. 2006;105(2):294-300.
- Rubino PA, Rhoton AL Jr, Tong X, Oliveira E. Three-dimensional relationships of the optic radiation. *Neurosurgery*. 2005;57(4 suppl):219-227; discussion 219-227.
- Gungor A, Baydin S, Middlebrooks EH, Tanriover N, Isler C, Rhoton AL Jr. The white matter tracts of the cerebrum in ventricular surgery and hydrocephalus. *J Neurosurg*. 2016;1-27. [epub ahead of print]
- Sampath R, Katira K, Shi R, Vannemreddy P, Patil S, Nanda A. Radio-anatomic measurements and statistical generation of a safe surgical corridor to enter the ventricular trigone while avoiding injury to the optic radiations. *J Neurol Surg A Cent Eur Neurosurg*. 2014;75(6):453-461.
- Mahaney KB, Abdulrauf SI. Anatomic relationship of the optic radiations to the atrium of the lateral ventricle: description of a novel entry point to the trigone. *Neurosurgery*. 2008;63(4 suppl 2):195-202; discussion 202-193.
- Parraga RG, Ribas GC, Welling LC, Alves RV, de Oliveira E. Microsurgical anatomy of the optic radiation and related fibers in 3-dimensional images. *Neurosurgery*. 2012;71(1 suppl operative):160-171; discussion 171-162.
- Wu W, Rigolo L, O'Donnell LJ, Norton I, Shriver S, Golby AJ. Visual pathway study using in vivo diffusion tensor imaging tractography to complement classic anatomy. *Neurosurgery*. 2012;70(1 suppl operative):145-156; discussion 156.
- Ebeling U, Reulen HJ. Neurosurgical topography of the optic radiation in the temporal lobe. *Acta Neurochir (Wien)*. 1988;92(1-4):29-36.
- Ono M, Kubik S, Abernathy CD. *Atlas of the Cerebral Sulci*. New York: Thieme; 1990.
- Petrides M. *The Human Cerebral Cortex: An MRI Atlas of the Sulci and Gyri in MNI Stereotaxic Space*. London: Elsevier/Academic Press; 2012.
- Ribas GC. The cerebral sulci and gyri. *Neurosurg Focus*. 2010;28(2):1-24.
- Jensen J. Die Furchen und Windungen der menschlichen Großhirnhemisphären. *Allgemeine Zeitschrift für Psychiatrie und Psychisch*. 1871;27:473-516.
- Klingler J, Ludwig E. *Atlas Cerebri Humani*. Basel, NY: Karger; 1956.
- Koutsarnakis C, Liakos F, Kalyvas AV, Sakas DE, Stranjalis G. A laboratory manual for stepwise cerebral white matter fiber dissection. *World Neurosurg*. 2015;84(2):483-493.
- Koutsarnakis C, Liakos F, Liouta E, Themistoklis K, Sakas D, Stranjalis G. The cerebral isthmus: fiber tract anatomy, functional significance, and surgical considerations. *J Neurosurg*. 2016; 124(2): 450-462.
- Yasargil MG. A legacy of microneurosurgery: memoirs, lessons, and axioms. *Neurosurgery*. 1999;45(5):1025-1092.
- Yasargil MG. *Microneurosurgery*. Vol 4A. Stuttgart: Thieme; 1994.
- Yasargil MG. *Microneurosurgery*. Vol 4B. Stuttgart: Thieme; 1996.
- Yasargil MG. *Microneurosurgery*. Vol 1. Stuttgart: Thieme; 1984.
- Yasargil MG, Cravens GF, Roth P. Surgical approaches to "inaccessible" brain tumors. *Clin Neurosurg*. 1988;34:42-110.
- Harkey HL, al-Mefty O, Haines DE, Smith RR. The surgical anatomy of the cerebral sulci. *Neurosurgery*. 1989;24(5):651-654.
- Pia HW. Microsurgery of gliomas. *Acta Neurochir (Wien)*. 1986;80(1-2):1-11.
- Ribas G C, Yasuda A, Ribas EC, Nishikuni K, Rodrigues AJ Jr. Surgical anatomy of microneurosurgical sulcal key points. *Neurosurgery*. 2006;59(4 suppl 2):ONS177-ONS210; discussion ONS210-ONS171.
- Bertalanffy H, Krayenbuhl N, Wess C, Bozinov O. *Ventricular Tumors. Neurological Surgery*, 6th edn. Saunders: Elsevier; 2011.
- Nakamura M, Roser F, Bundschuh O, Vorkapic P, Samii M. Intraventricular meningiomas: a review of 16 cases with reference to the literature. *Surg Neurol*. 2003;59(6):491-503; discussion 503-494.
- Fornari M, Savoiaro M, Morello G, Solero CL. Meningiomas of the lateral ventricles. Neuroradiological and surgical considerations in 18 cases. *J Neurosurg*. 1981;54(1):64-74.
- Izci Y, Seckin H, Ates O, Baskaya MK. Supracerebellar transtentorial transcolateral sulcus approach to the atrium of the lateral ventricle: microsurgical anatomy and surgical technique in cadaveric dissections. *Surg Neurol*. 2009;72(5):509-514; discussion 514.
- Brodman K. *Vergleichende Lokalisationslehre der Grobhirnrinde*. Leipzig: Barth; 1909:13.
- Connolly CJ. *External Morphology of the Primate Brain*. Illinois: CC Thomas; 1950.

37. Critchley M. *The Parietal Lobes*. London: Edward Arnold; 1953:1-61.
38. Dejerine J. *Anatomie des Centres Nerveux*. Masson edition 1980. Paris: Rueff et Cie; 1895:233-290.
39. Eberstaller O. Zur Oberflächen-Anatomie der Grosshirn-Hemisphären. *Wien Med Blätter*. 1884;7:610-616.
40. Testut L, Jacob O. *Topographic Anatomy Textbook*, edn 5. Barcelona: Salvat; 1932.
41. von Economo CF, Parker S. *The Cytoarchitectonics of the Human Cerebral Cortex*. London: Humphrey Milford; 1929.
42. Williams PL, Warwick R. *Functional Neuroanatomy of Man: Being the Neurology Section From Gray's Anatomy*. London: Churchill Livingstone; 1975.
43. Ebeling U, Steinmetz H. Anatomy of the parietal lobe: mapping the individual pattern. *Acta Neurochir (Wien)*. 1995;136(1-2):8-11.
44. Zlatkina V, Petrides M. Morphological patterns of the intraparietal sulcus and the anterior intermediate parietal sulcus of Jensen in the human brain. *Proc Biol Sci*. 2014;281(1797):1-8.
45. Duffau H, Capelle L, Sichez N, et al. Intraoperative mapping of the subcortical language pathways using direct stimulations. An anatomico-functional study. *Brain*. 2002;125(pt 1):199-214.
46. Fernandez-Miranda JC, Rhoton AL Jr, Alvarez-Linera J, Kakizawa Y, Choi C, de Oliveira EP. Three-dimensional microsurgical and tractographic anatomy of the white matter of the human brain. *Neurosurgery*. 2008;62(6 suppl 3):989-1026; discussion 1026-1028.
47. Spina G, Gatignol P, Capelle L, Duffau H. Superior longitudinal fasciculus subserves vestibular network in humans. *Neuroreport*. 2006;17(13):1403-1406.
48. Kato I, Sato S, Watanabe S, Nakashima H, Takeyama I, Watanabe Y. Role of the dorsolateral pontine nucleus in two components of optokinetic nystagmus (OKN). *Acta Otolaryngol Suppl*. 1993;504:7-12.
49. Wakana S, Jiang H, Nagae-Poetscher LM, van Zijl PC, Mori S. Fiber tract-based atlas of human white matter anatomy. *Radiology*. 2004;230(1):77-87.
50. Turken AU, Dronkers NF. The neural architecture of the language comprehension network: converging evidence from lesion and connectivity analyses. *Front Syst Neurosci*. 2011;5:1-20.
51. Catani M, Jones DK, Ffytche DH. Perisylvian language networks of the human brain. *Ann Neurol*. 2005;57(1):8-16.
52. Catani M, Mesulam M. The arcuate fasciculus and the disconnection theme in language and aphasia: history and current state. *Cortex*. 2008;44(8):953-961.
53. Kamada K, Todo T, Masutani Y, et al. Visualization of the frontotemporal language fibers by tractography combined with functional magnetic resonance imaging and magnetoencephalography. *J Neurosurg*. 2007;106(1):90-98.
54. Makris N, Kennedy DN, McInerney S, et al. Segmentation of subcomponents within the superior longitudinal fascicle in humans: a quantitative, in vivo, DT-MRI study. *Cereb Cortex*. 2005;15(6):854-869.
55. Young PA, Young PH. *Basic Clinical Neuroanatomy*. Williams & Wilkins; 1997.
56. Kahane P, Hoffmann D, Minotti L, Berthoz A. Reappraisal of the human vestibular cortex by cortical electrical stimulation study. *Ann Neurol*. 2003;54(5):615-624.
57. Grefkes C, Fink GR. The functional organization of the intraparietal sulcus in humans and monkeys. *J Anat*. 2005;207(1):3-17.
58. Hutchinson JB, Uncapher MR, Weiner KS, et al. Functional heterogeneity in posterior parietal cortex across attention and episodic memory retrieval. *Cereb Cortex*. 2014;24(1):49-66.
59. Binkofski F, Dohle C, Posse S, et al. Human anterior intraparietal area subserves prehension: a combined lesion and functional MRI activation study. *Neurology*. 1998;50(5):1253-1259.
60. Frey SH, Vinton D, Norlund R, Grafton ST. Cortical topography of human anterior intraparietal cortex active during visually guided grasping. *Brain Res Cogn Brain Res*. 2005;23(2-3):397-405.
61. Mars RB, Jbabdi S, Sallet J, et al. Diffusion-weighted imaging tractography-based parcellation of the human parietal cortex and comparison with human and macaque resting-state functional connectivity. *J Neurosci*. 2011;31(11):4087-4100.
62. Shikata E, McNamara A, Sprenger A, et al. Localization of human intraparietal areas AIP, CIP, and LIP using surface orientation and saccadic eye movement tasks. *Hum Brain Mapp*. 2008;29(4):411-421.
63. Caminiti R, Chafee MV, Battaglia-Mayer A, Averbeck BB, Crowe DA, Georgopoulos AP. Understanding the parietal lobe syndrome from a neurophysiological and evolutionary perspective. *Eur J Neurosci*. 2010;31(12):2320-2340.
64. Battaglia-Mayer A, Caminiti R. Optic ataxia as a result of the breakdown of the global tuning fields of parietal neurones. *Brain*. 2002;125(pt 2):225-237.
65. Perenin MT, Vighetto A. Optic ataxia: a specific disruption in visuomotor mechanisms. I. Different aspects of the deficit in reaching for objects. *Brain*. 1988;111(pt 3):643-674.
66. Greene JD. Apraxia, agnosias, and higher visual function abnormalities. *J Neurol Neurosurg Psychiatry*. 2005;76(suppl 5):v25-v34.
67. Villa G, Gainotti G, De Bonis C. Constructive disabilities in focal brain-damaged patients. Influence of hemispheric side, locus of lesion and coexistent mental deterioration. *Neuropsychologia*. 1986;24(4):497-510.
68. Roux FE, Dufor O, Lauwers-Cances V, et al. Electrostimulation mapping of spatial neglect. *Neurosurgery*. 2011;69(6):1218-1231.
69. Corbetta M, Shulman GL. Spatial neglect and attention networks. *Annu Rev Neurosci*. 2011;34:569-599.
70. Heilman KM, Valenstein E, Watson RT. Neglect and related disorders. *Semin Neurol*. 2000;20(4):463-470.
71. Vaessen MJ, Saj A, Lovblad KO, Gschwind M, Vuilleumier P. Structural white-matter connections mediating distinct behavioral components of spatial neglect in right brain-damaged patients. *Cortex*. 2016;77:54-68.
72. Thimm M, Fink GR, Kust J, Karbe H, Willmes K, Sturm W. Recovery from hemineglect: differential neurobiological effects of optokinetic stimulation and alertness training. *Cortex*. 2009;45(7):850-862.

## COMMENTS

The authors provide a valuable contribution to those caring for patients with intraaxial and intraventricular (atrial) tumors. An intraparietal sulcus approach yields access to deep white matter tumors as well as to the atrium of the ventricle. The authors perform a critical analysis of the white matter tracts encountered in this approach and verify that a mid sulcus approach vs a IPS/postcentral should spare the arcuate segment of the superior longitudinal fasciculus, a finding not previously recognized. They also document the cognitive deficits expected with such an approach. Superior parietal lobe cognitive deficits are typically more severe in the non-dominant parietal lobe than the dominant parietal lobe.

As surgeons, we balance the need to obtain as great an extent of resection as possible with the risks of neurologic deficits. Frequently, we have to make a choice to get to a tumor by going through brain and for this reason, we perform surgery with a variety of mapping techniques including SSEPs, direct cortical stimulation sometimes with the patient awake. Certain tracts and their respective functions are difficult to map and thus any additional information in advance of transecting fibers is very useful to have. The intraparietal sulcus approach should be part of the neurosurgeon's armamentarium to reach the ventricle and this article documents the specifics of tract localization and methods to minimize deficits. I congratulate the authors and this work and their contribution to our understanding of the white matter tracts encountered on the way to the atrium of the ventricle.

**Jeffrey S. Weinberg**  
Houston, Texas